

Development of a Conceptual Design Tool for Supersonic Transport with a Variable Fidelity Interface

T. Dietl¹, S. Schnell², P. Shiva Prakasha¹, B. Nagel¹, O. Brodersen²

German Aerospace Center (DLR);

¹Institute of System Architectures in Aeronautics, Hamburg, Germany;

²Institute of Aerodynamics and Flow Technology, Braunschweig, Germany

Abstract

The growing attention of supersonic transport (SST) renews economic and environmental concerns. New designs shall improve flight efficiency as well as mission, air traffic management (ATM) & air traffic service (ATS) impact, requiring a flexible and collaborative approach. A conceptual design tool linking to varied fidelity domain is developed in DLR since 2005. The focus areas of this paper are:

- Expanding openAD to design and evaluate future SST Aircraft within a higher-fidelity workflow
- Capabilities demonstration of openAD via sensitivity studies of reference vehicle Concorde, HIASC A, HICAC C and X-59A (publicly available data)

Keywords: Conceptual Aircraft Design, Supersonic Transport

1. MOTIVATION

19 years after the Concorde made its final commercial flight, the field of supersonic transport (SST) is rising attention again, promising a significant reduction in travel time comparable to today's airliners [1] [2]. Ongoing research programs and funding predict a future market potential of commercial supersonic flight under the condition of unrestricted flight paths [3]. Nevertheless, the impact at mission level, ATM level and ATS level and on the environment shall be minimized by the design of very efficient and quiet configurations.

Research institutes around the world are proposing new methods for the design of a future supersonic transport vehicle. Topics like transonic and supersonic aerodynamic modeling by Krus and Abdalla [4], sonic boom prediction by Ding et al. [5] or conceptual sizing formulas based on extant supersonic designs by Joiner et al. [6] as well as concepts for supersonic transport were addressed. The focus there is on the design of supersonic business jets (SSBJ). Berton et al. introduces two simple 55t and a 45t concept to evaluate take-off and landing noise and procedures [7]. Abdalla et. al. evaluates the aerodynamic capabilities of a variable half-span SSBJ [8]. There is a high focus on low-boom capabilities of concepts, mentioning the sonic boom stealth concept of Sun and Smith et al. [9] and the low boom design evaluated for environmental impact by ONERA [10]. Another big topic within supersonic commercial flying is landing and take-off (LTO) noise studied by Nöding [11]. Besides that, Lawrence et al. evaluates a different class with a configuration of 200 passenger at Mach 3.0 with a CFD wing shape optimization [12]. Previous work in preliminary supersonic aircraft design was performed by Seubert et al., who extended the Preliminary Aircraft Design and Optimization tool (PrADO)

of the Technical University of Braunschweig for SST [13]. Based on that, the DLR in cooperation with the TU Braunschweig has carried out various work on supersonic preliminary design [14].

For this newly established need to assess supersonic configurations, a flexible and collaborative design approach is desired. This approach needs to be able to all design disciplines, but also answer questions on fleet level. The conceptual aircraft design tool "OpenAD", which links to other domain with varied fidelity, is developed in DLR since 2005. In order to design and analyze advanced supersonic concepts while integrating new technologies, the design tool has been extended for supersonic configuration design. This paper describes the enhancements in mission design, mass estimation, aerodynamic modeling, stability calculation, engine performance and geometrical modeling for supersonic preliminary aircraft design. After the description of the extensive method selection, their results are validated for supersonic reference aircraft. The methods are selected to sufficiently describe all disciplines, but most importantly to meet the overall aircraft parameters in order to create holistic and inherently consistent concepts. The tool can be used as a standalone tool, offering the user high flexibility and easy access to vary and optimize parameters. The output in a standard (Common Language for Aircraft Design) CPACS format allows implementation in a broader design environment, which is already planned for the future. In order to implement results of higher-fidelity tools, it is possible to activate and deactivate modules, based on the provided input. Together with the work of Froehler et al [15], this extends the flexibility by enabling openAD to calculate a broad variety of air transportation vehicles from conventional configurations over Blended-wing-body (BWB) to SST, as displayed in FIGURE 1.

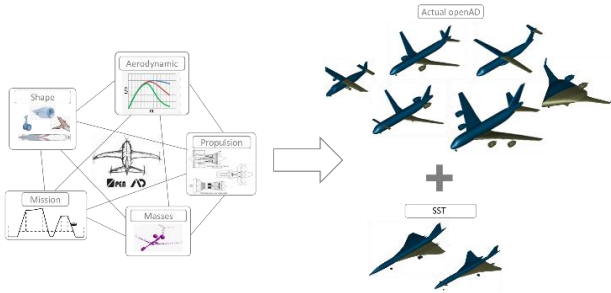


FIGURE 1: Design Space Extension in openAD

OpenAD now can be applied to overall aircraft calculation, design space exploration and parameter optimization within a validated supersonic design space between Mach numbers from 1.2 to 2.0, a range between 500 nm and 4000 nm up to a cruise altitude of 17 km. Besides Supersonic Business Jets and Commercial Supersonic Transport (CSST) aircraft, experimental aircraft are considered for the validated design space in order to benefit from a broader base of comparable applications supported with real world data. Therefore, seating capacities from 1 to 108 with various configurations like T-tails, canards and fuselage mounted engines, with engine numbers from one to four are validated. The capabilities are shown by a sensitivity study of a Concorde-similar concept. The supersonic version of openAD is already successfully applied in current research projects.

2. GENERAL STRUCTURE AND INITIAL STATE OF OPENAD

The supersonic capabilities are an enhancement of the conventional openAD. It is a software tool for conceptual aircraft design written in Python scripting language. Within the tool, well-known and mostly publicly obtainable handbook methods [16] [17] [18] [19] [20] [21] are completed by own methods, where no adequate models could be found in public literature. It has an object-oriented structure and is therefore highly flexible, allowing fast extensions to the knowledge base. The tool reads an XML file as an input, where all parameters within the knowledge space can be adjusted in value and calculation status. In order to enable exchangeability of information between openAD and higher-fidelity tools in order to implement collaborative workflows, results are exported as XML file in a CPACS compatible format as described by Alder et al [22]. Further information about the structure of openAD can be found in [23].

The validated design space of subsonic openAD is 19 up to 800 passengers. It is designed for BWB and tube and wing configurations with various options like T-tails, canards, fuselage mounted engines, for turbofan, turboprop and distributed propulsion [23] [15].

3. ADAPTIONS TO SUPERSONIC DESIGN

In order to make the necessary changes in the calculation methods for openAD, the design space for SSTs to be calculated needs to be specified first. The design space is defined on the basis of top-level aircraft requirements (TLARs) and requirements by the openAD development team. It is also based on current literature [24], [2].

Current use cases are the single seat aircraft X-59A with a Canard and tail configuration, a SSBJ with Canard configuration and one with conventional tail, each for 8 seats as well as a Concorde similar CSST for 100 Pax. These use cases are presented in FIGURE 2.

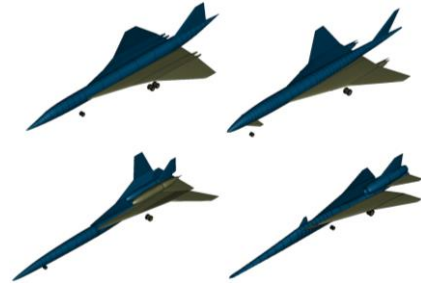


FIGURE 2: Implemented supersonic use cases (Concorde, HISAC A, HISAC C, X-59A)

The parameters shown in TAB 1 describe the design space for SST. It has to be mentioned that the shown parameter ranges are not fixed boundaries. Depending on the methods used, the design space can be greater than the given parameter ranges. Therefore, further method verification is necessary.

TAB 1: Design space of openAD for SST

Parameter	Range
Mach Number	1.2 - 2.0
Design Range	500 – 6000 nm
Cruise Altitude	< 17 km
Aircraft Types	SSBJ, CSST
Seating Capacity	1 - 110
Aircraft Configurations	Canard, conventional tail, Delta-wing, Canard & tail

Based on the design space, important design methods and parameter for SST aircraft design have to be determined. In the following, they will be compared to the already implemented aircraft design methods in openAD and adapted or added if necessary. All relevant topics not covered in this paper regarding general aircraft design can be found in Woehler [23]. In order to maintain the general code structure of openAD as well as short calculation times, low-fidelity methods such as handbook and empirical methods are used. All methods are validated with reference aircraft as described in chapter 4.

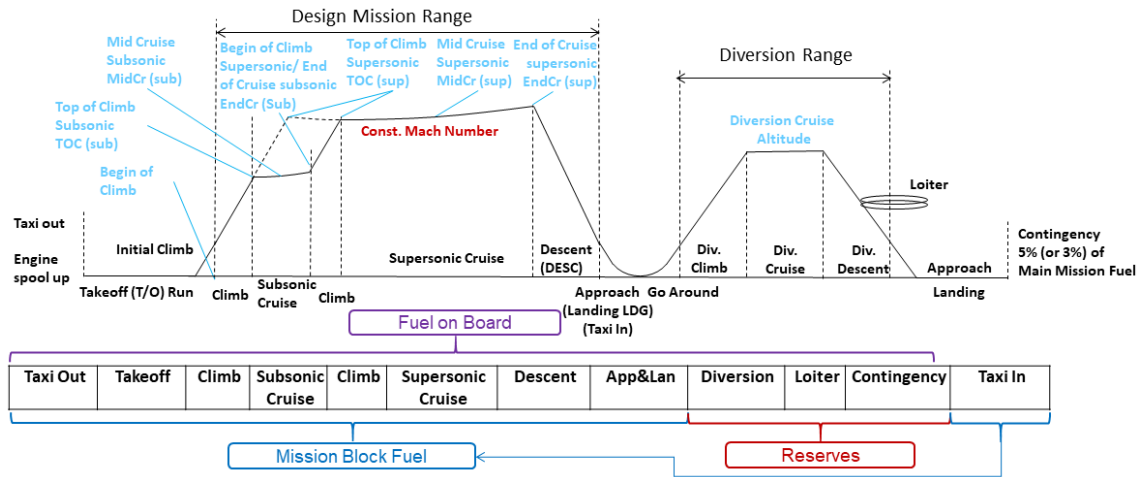


FIGURE 3: Standard mission profile [27] with additional subsonic cruise

The design methods and parameters which have to be analyzed include standard design mission, mass estimation, aerodynamic modelling, stability calculation, engine performance and geometry adaptations. Further design properties like sonic-boom, airport noise and emission will be considered in future work or by other parts of the toolchain mentioned in chapter 2.

3.1. Standard Design Mission

It is expected, that a relevant number of cruise flights performed by SST will begin or end over land and therefore have limits in their cruise speed [2]. To consider this, the standard design mission of openAD is extended by an additional cruise segment for subsonic cruise.

The mission profile is the base of the mission fuel calculation. It is the standard National Business Aviation Association (NBAA) mission profile and can be used in two different variants aligned with Gonzalez-Gallego et al [25], presented in FIGURE 3, symbolizing the standard mission profile in pointed dots. SST vehicles based on that mission will require low-boom capabilities and a relaxation over overland sonic boom regulations. It is described in detail in [23]. FIGURE 3 also shows an additional subsonic cruise phase. This profile enables supersonic cruise under today's regulations, but forces the vehicle to operate in off-design conditions for a longer period of time. That makes the following units for fuel and performance calculation necessary:

- Subsonic climb from begin of climb at 1500 ft to top of climb of initial subsonic cruise altitude
- Subsonic cruise from top of climb at 30000 ft [26] to the begin of climb to supersonic cruise
- Climb from end of supersonic cruise to top of climb at initial cruise altitude
- Supersonic cruise from end of climb at cruise Mach number – 0.02 till start of descent

The acceleration through Mach 1 is covered in greater detail in chapter 3.

3.2. Mass Estimation

The implemented mass estimation methods of openAD are

tested with supersonic reference aircraft. Because some methods are not applicable with deviations between the conventional openAD results and the literature values, some methods are revised. For each component, different methods are evaluated and compared between each other and to the already implemented method. To be applied as default, a model needs to deliver reasonable results over the full range of the reference aircraft. That shows applicability also for aircraft evaluated in the future in sizes between the reference aircraft. For example, the evaluation of the engine weight method is demonstrated in TAB 2.

TAB 2: Engine weight method deviations

Reference	Literature [kg]	Conventional openAD	Raymer	Svodoba	Nijsse
Concorde	2952 [27]	-57,93%	-28,67%	15,22%	-74,00%
HISAC A	confidential	-48,30%	-26,18%	27,97%	-68,23%
HISAC C	confidential	-44,29%	22,97%	120,40%	-43,02%

Even though Raymer's method is not the best for every aircraft displayed here, it delivers the best results over the course of all aircraft. It has the minimal average and no extreme deviation. Therefore, Raymer's engine weight method is selected. This leads to adjustments for fuselage structure, nose gear and wing structural mass estimations.

3.3. Aerodynamic Modelling

The main aspect of aerodynamic modelling for preliminary aircraft design is a sufficiently suitable supersonic drag coefficient estimation in several points of the flight envelope. Therefore, different handbook methods are compared using literature values of reference aircraft. The analysis shows, that none of the methods is sufficient for all reference aircraft and flight conditions. Therefore, in openAD a mixed approach of the Raymer and Nicolai method is implemented. The drag breakdown of openAD is as described below:

$$(1) \quad c_D = c_{D0} + c_{Di} + c_{Dw}$$

Where: c_D is the total drag coefficient of the aircraft

c_{D0} is the zero-lift drag coefficient

c_{Di} is the lift-dependent drag coefficient

c_{Dw} is the wave drag coefficient [23]

They are separately described in the following.

3.3.1. Zero-lift drag coefficient

The zero-lift drag coefficient is calculated by the method of Nicolai [28].

$$(2) \quad c_{D0} = \sum_{i=0}^n \frac{C_{f_i} \times FF_i \times S_{wet_i}}{S_{ref}}$$

Where C_{f_i} is the skin friction coefficient, FF_i is the form factor and S_{wet_i} is the wetted area of each component i . The formula is valid for supersonic as well as subsonic speeds.

3.3.2. Lift-dependent drag coefficient

For the lift-dependent drag coefficient at subsonic speeds, the already implemented method (3) of openAD is used. For supersonic speeds, a factor K is calculated and multiplied with the square of c_L (4).

$$(3) \quad c_{Di} = c_L \times li + \frac{1}{AR \times \pi \times Oswald} c_L^2 + \Delta c_{DpolarBreak}$$

$$(4) \quad c_{Di} = K \times c_L^2$$

K is the drag due to lift factor, its calculation can be seen in Raymer [21] and $\Delta c_{DpolarBreak}$ is the airfoil drag penalty above a certain c_L -Value, following a cubic polynom. The polynom is derived to follow the drag increase of a NACA 24018 airfoil after a polar break c_L of 0.4.

3.3.3. Wave drag coefficient

The following formula (5) is used to approximate the wave drag coefficient for $Ma \geq 1.2$:

$$(5) \quad c_{Dw} = 1.5 \times \left[1 - 0.386 \times (Ma - 1.2)^{0.57} \times \left(1 - \frac{\pi \times \varphi_{LE}^{0.77}}{100} \right) \right] \times \frac{9\pi}{2} \left(\frac{A_{max}}{l_{fus}} \right)^2 / S_{ref}$$

Where A_{max} is the max cross-sectional area, l_{fus} is the fuselage length and φ_{LE} is the wing leading edge angle. The wave drag coefficient for $Ma < 1.2$ is approximated by a Bezier-Curve according to the method of Raymer [21].

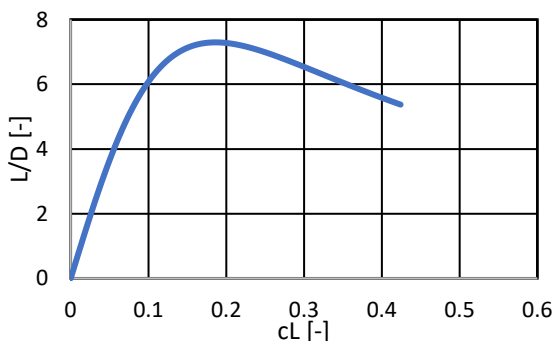


FIGURE 4: Clean lift-over-Drag Polar of the Concorde similar aircraft

With these adaptations, the reference aircraft are recalculated. The result of the openAD aerodynamic clean Lift-over-Drag polar calculation for the Concorde similar configuration is presented in FIGURE 4. FIGURE 5 shows

the calculated drag coefficients of a Concorde similar aircraft over the Mach number for a given altitude.

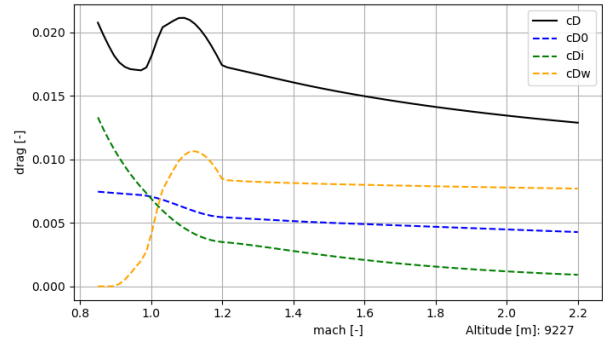


FIGURE 5: Drag vs. Mach number of a Concorde similar aircraft

3.4. Stability Calculation

The stability calculation of the supersonic part of openAD mainly considers the longitudinal static stability, driven by neutral point and center of gravity (CG) position. As a first approach of the preliminary design, it is assumed that the aerodynamic center of the wings is at 25% of the mean aerodynamic chord (MAC) for subsonic and at 50% for supersonic flight [21]. For the Neutral Point (NP) calculation, a distinction between conventional tail, Canard, no tail and a Canard and tail configuration is done. Thus, openAD is able to calculate a wide range of aircraft configurations. The underlying calculation methods are [29] for conventional tail or no tail, [30] for Canard and [31] for the Canard and tail configuration.

The methods consider the static longitudinal stability regulations [32] of positive static margin over all mission phases, with NP located in front of the CG as displayed in FIGURE 6.

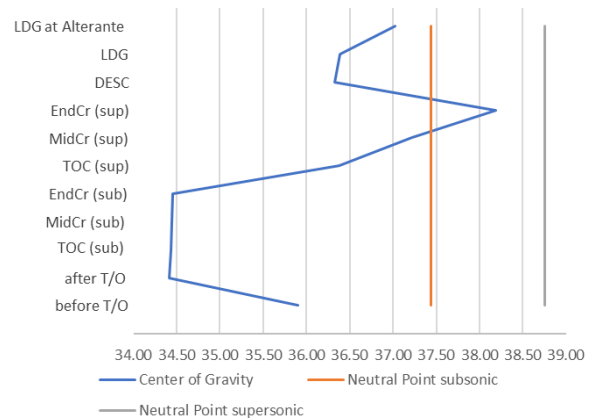


FIGURE 6: Center of Gravity shift of a Concorde similar aircraft

Following that rule the wing is positioned automatically with respect to positive static margin in all flight phases. That is especially critical during the subsonic flight phases. It can be influenced by a user-given minimum static margin. A maximum static margin is not considered automatically, but the static margin of each mission point is an output and can therefore be checked by the user manually. The CG

movement over the course of the flight is heavily impacted by the fuel CG. Active CG control is considered by fuel pumping between the different tanks. With that in mind the center wing tank can be divided into two units to have a higher impact on CG. The order in which fuel tanks are emptied can be adjusted by the user for every flight phase with respect to the configuration of the aircraft. A trim tank can be used to avoid too stable conditions in supersonic flight. More to the geometry of fuel tanks can be read in chapter 3.6.

3.5. Engine Performance

The engine model of subsonic openAD is not applicable for supersonic. Since calculating own engine decks is not necessary, because they will be delivered by partners, a simplified engine model is sufficient for initial design and thrust requirements definition. The main interest for conceptual design lays in specific fuel consumption (SFC) and thrust prediction for different altitudes and Mach numbers. For both the methodology by Howe [33] is applied. They offer quick estimation with reduced complexity over different flight phases.

3.5.1. Specific fuel consumption estimation

The necessary input parameters are:

- Reference factor to given powerplant C'
- Bypass ratio (BPR)
- Flight Mach Number (Ma)
- Altitude in the form density ratio $\sigma_{ALT} = \frac{\rho_{ALT}}{\rho_0}$

The method depends on the use of an afterburner. Dry conditions are calculated via (6), wet conditions via (7).

$$(6) \quad SFC = C' \times (1 - 0.15 \times BPR^{0.65}) \times [1 + 0.28 \times (1 + 0.63 \times BPR^2) \times Ma] \times \sigma^{0.08}$$

As additional input (7) needs

- Thrust in wet conditions (TW)
- Thrust in dry condition (TD)

$$(7) \quad SFC = 1.05 \times \left(\frac{TW}{TD}\right) \times (1 + 0.17 \times Ma) \times \sigma^{0.08}$$

SFC can be calibrated either by a global SFC calibration factor or for each flight phase individually.

3.5.2. Thrust estimation

For thrust calculation a base information about the thrust at International Standard Atmosphere (ISA) conditions at sea level F_{ISA} is necessary, if there is no sufficient information about a comparable engine available openAD assumes that information based on the needs of the most thrust critical flight phase. Additional input parameters are:

- Bypass ratio (BPR)
- Flight Mach Number (Ma)
- Altitude in the form density ratio $\sigma_{ALT} = \frac{\rho_{ALT}}{\rho_0}$

The powerplant thrust parameters $K_{1\tau}$, $K_{2\tau}$, $K_{3\tau}$, $K_{4\tau}$, S depend on BPR , Ma and operating conditions wet or dry are assumed to be constant for a defined range of Mach number and operating conditions. They are listed in [33].

Below Mach 0.9 thrust F is calculated by (8).

$$(8) \quad F = F_{ISA} \times [K_{1\tau} + K_{2\tau} \times BPR + (K_{3\tau} + K_{4\tau} \times BPR) \times Ma] \times \sigma_{ALT}^S$$

Above Mach 0.9 (9) is applied:

$$(9) \quad F = F_{ISA} \times [K_{1\tau} + K_{2\tau} \times BPR + (K_{3\tau} + K_{4\tau} \times BPR) \times (Ma - 0.9)] \times \sigma_{ALT}^S$$

The SFC and thrust methods need to be calibrated to the design point of the engine, therefore there is no deviation at the cruise point. Calibration can be performed via a global calibration factor, as applied for values above. If more specific information about an engine is available via calibration can be performed for each flight phase individually.

The higher the Mach number the more precise the SFC estimations are. The bigger deviations in the lower segments are acceptable since the cruise is the by far dominating segment. It is recommended to define the static thrust at sea level as an input parameter, when recalculating existing aircraft. Calibration to a reference aircraft is recommended due to relatively high deviations.

To give visual feedback to the aircraft designer, openAD now returns a plot of the available and required thrust, Mach number and altitude for the mission points from take-off until end of cruise. Remaining mission points are not dimensioning for the thrust demand and can be neglected here. The thrust plots of openAD for a Concorde similar aircraft can be seen in FIGURE 7.

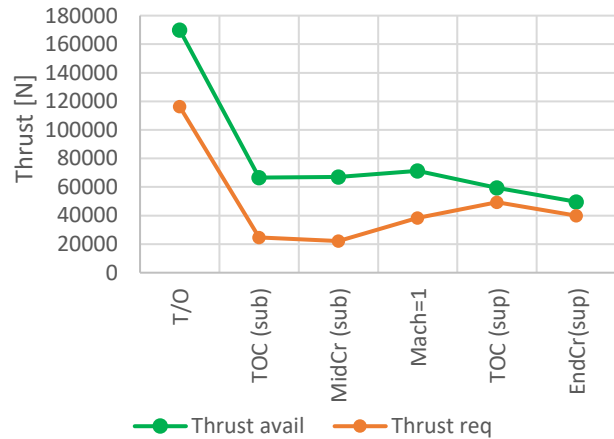


FIGURE 7: Available and required thrust for several mission points for a Concorde similar aircraft

3.6. Geometry

The different configuration aspects of supersonic vehicles lead geometrical aspects which do not need to be considered in the subsonic but supersonic aircraft design. This includes other limitations to the landing gear dimensions, additional fuselage fuel tanks, trim tank, the delta wing structure and wing fuel capacity. Additional configurations options are one engine design and three-surface -aircraft implementation. OpenAD is set to design a conventional aircraft configuration. Changes deviating of the conventional configuration can be defined in the tool

input. Deviations like additional vertical surfaces can be controlled via individual switches and an appropriate location has to be chosen in the input selection. Each component will be adjusted due to the parametrization.

3.6.1. Fuselage Geometry

The fuselage geometry definition is based on an inside out approach where the cockpit, cabin definition and fuselage fuel tank is sizing length and height. Typical fuselages of supersonic aircraft differ from those of subsonic aircraft mainly by a long nose and tail as well as their slenderness. Therefore, in openAD new fuselage geometries for the X-59A and the Concorde are now available. They can be seen in FIGURE 12, FIGURE 15 and FIGURE 18. A wave drag optimized fuselage shape is not intended in this design phase because it is part of the further aircraft design optimization.

3.6.2. SSBJ Cabin definition

The fuselage length is defined by several sections like nose tail, cabin and trim tank. Business jet cabins can have a unique cabin layout. In order to be able to predict cabin lengths l_{cabin} below 19 seats better the following equations is created by a statistical approach based on the number of passenger seats and divided by range via the data from [34]. (10) is applied for a design range below 3500 km and (11) over.

$$(10) \quad l_{cabin} = 0,6083 \times Seats_{pax} + 0,6954$$

$$(11) \quad l_{cabin} = 1,4818 \times Seats_{pax} - 4,5078$$

3.6.3. Landing Gear

The landing gear height is mainly driven by side and rear clearance angle. The rear clearance angle of conventional aircraft is usually determined by the lift of angle between fuselage and ground at lift of rotation. An additional constraint by the engines is implemented by example of the Concorde, where the limiting factor is not a tail strike but a strike of the engine nozzle as shown in FIGURE 8. The Concorde is equipped with an extended tail bumper in order to prevent engine damage.



FIGURE 8: Engine as Concorde tail strike requirement

3.6.4. Wing Fuel Tank

Up to this point openAD assumed the space between the front and rear spar as a fuel storage. While this is a valid assumption for conventional high aspect ratio wings used in conventional subsonic airliners, it does not apply to the widely used delta wing for supersonic use cases. Displayed as an example you can see the fuel tank arrangement of the Concorde in FIGURE 9.

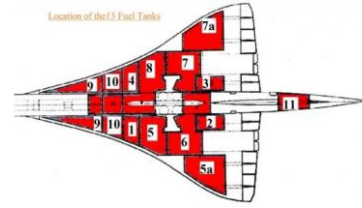


FIGURE 9: Concorde fuel tank location [35]

The new calculation method requires a calibration assumes the whole wing to be available for fuel storage. While space for wing structure and flaps are considered, the calibration of the maximum fuel storage to an applicable reference aircraft is recommended for new designs. In order to influence CG movement during emptying the tanks over the course of the flight, the center tank can be divided into two separate parts.

3.6.5. Fuselage Fuel Tank

Due to the high fuel fraction and flat wings of SST fuel capacity is a relevant problem, especially in the class of SSBJ. To solve that problem fuselage fuel tanks are often used to increase fuel capacity. In openAD the main fuselage tank is located between vertical tail plane (VTP) attachment and the end of the cabin. If the fuselage fuel tank option is enabled the geometry is calculated based on the fuselage diameter and the additional necessary fuel volume. It can also be configured directly by the designer.

3.6.6. Trim Tank

The already mentioned stability challenges often lead to the necessity of a trim tank. A trim tank is considered in the tail of the fuselage marked red in FIGURE 10.

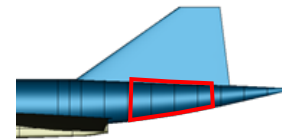


FIGURE 10: Trim Tank implementation in openAD

Volume calculation is based on the available volume between beginning and end of the trim tank. Position and length calculation of the trim tank are based on statistics, but due to the high individuality of supersonic designs and the small knowledge space, direct input of the designer is advised. The fuel capacity of the trim tank is not included into the maximum fuel capacity of the aircraft.

3.6.7. Engine Geometry

The engine geometry is based on the available input. If no predefining input is given the engine diameter d_{ENG} is based on a methodology by Raymer [21], based on thrust at static ISA conditions at sea level and BPR in (12).

$$(12) \quad d_{ENG} = 0,288 \times \sqrt{F_{ISA}} \times e^{(0,04 \times BPR)}$$

Fan and nacelle diameter are calculated via a statistical approach derived from d_{ENG} .

Besides fan, engine and nacelle diameter their supersonic engines are often rectangular in order to influence flow

intake. This is dependent on the use of pylons as shown in FIGURE 11.

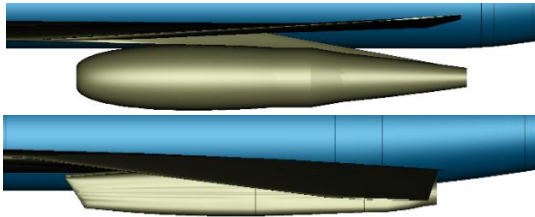


FIGURE 11: Engine Nacelle shapes

4. VALIDATION AND SENSITIVITIES

Chapter 3 states design capabilities for a design space from 1 to 110 passengers and a design cruise Mach number from 1.4 to 2.0. The following chapter provides results of supersonic reference aircraft calculation carried out by openAD. Aircraft characteristics for the reference aircraft are shown in TAB 3. Finally, sensitivities of weight, aerodynamic and engine efficiency for the Concorde similar aircraft are shown by alterations with respect to aircraft performance.

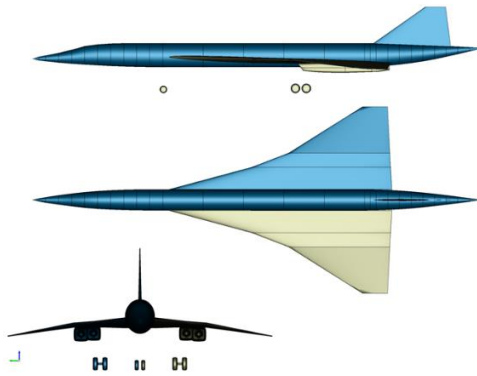


FIGURE 12: Three view Concorde similar aircraft

The selected reference aircraft cover a wide range of use cases and configurations. The Concorde, displayed in FIGURE 12 represents the classic airliner class aircraft. Even though it does not display today's technology standard, the limited availability of supersonic commercial aircraft makes it necessary to use the Concorde as a reference. Newer designs cannot provide operations data or have an overall limited availability of data. The aircraft

covers Mach numbers of around 2.0 in the long-range segment for around 100 seats with a delta wing configuration and defines the upper boundary of the design space validated in openAD for supersonic designs.

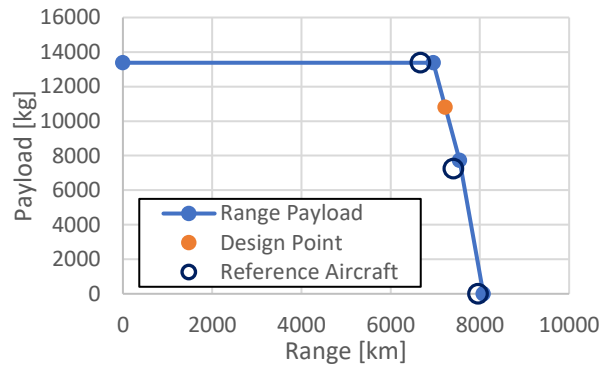


FIGURE 13: Payload-Range characteristics of a Concorde similar aircraft calculated by openAD compared to reference aircraft Concorde

The payload range characteristics of the Concorde similar aircraft are calculated in openAD and compared to reference data. The payload range diagram is especially suitable for this. The recalculated aircraft are set-up at their specific design point in openAD. The corner points are directly linked to the design weights, payload definition and maximum fuel capacity [16]. The slope of the substitution lines depends mainly on the aerodynamic and propulsion efficiency of the aircraft. The underlying aerodynamic performance calculated by openAD is exemplarily shown in FIGURE 4, FIGURE 17 and FIGURE 19 for the Concorde similar aircraft, the SSBJ and the experimental aircraft.

AS SSBJs the HISAC A and HISAC C represents the second common use case of supersonic commercial transport. The designs are the result of the European Project HISAC with the goal to investigate the possibility of a "Environmentally friendly high-speed aircraft [36]. The selected aircraft cover a wide range of configurations as presented in FIGURE 14 and FIGURE 15 within widely anticipated maximum take-off mass (MTOM) range for SSBJ of 50 t. HISAC A uses three engines, with one installed in the back and two below the wing as well as a canard and no horizontal tail plane (HTP). HISAC C has two installed engines within the tail and a conventional HTP and vertical tail plane (VTP) configuration. The results

TAB 3: Aircraft characteristics for the use cases presented

TLARs	Unit	Concorde [35]	HISAC A [36]	HISAC C [36]	X-59A [37]
Pax typical layout	[-]	108	8	8	0
Design Payload	[kg]	10800	760	730	272
Design Range	[NM]	3900	2915	3995	-
Design Cruise Mach Number	[-]	2.0	1.6	1.8	1.4
MTOM	[t]	185,0	51.1	53.3	11.3
Wing span	[m]	25.6	18.46	19.1	9.02
Number of engines	[-]	4	3	2	1

calculated in openAD are compared to reference data [36]. Due to the lack of availability of a payload range diagram more specific aircraft data are used. Especially suiting are overall aircraft descriptions like maximum take-off mass (MTOM), empty mass (EM) or operating empty mass (OEM) or lift-over Drag (L/D).

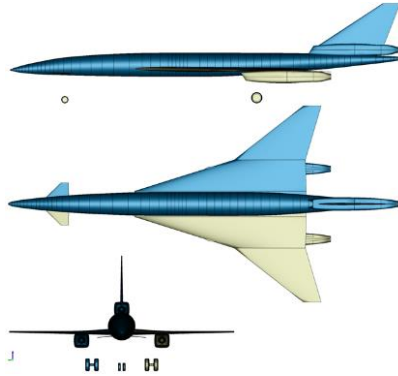


FIGURE 14: Three view HISAC A similar aircraft

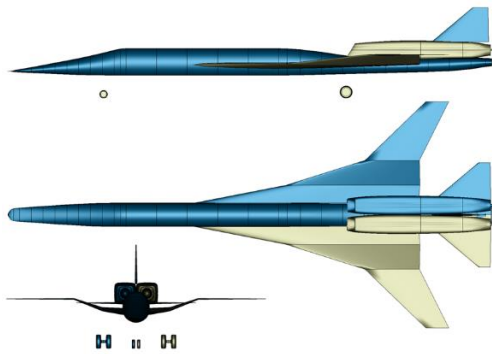


FIGURE 15: Three view HISAC C similar aircraft

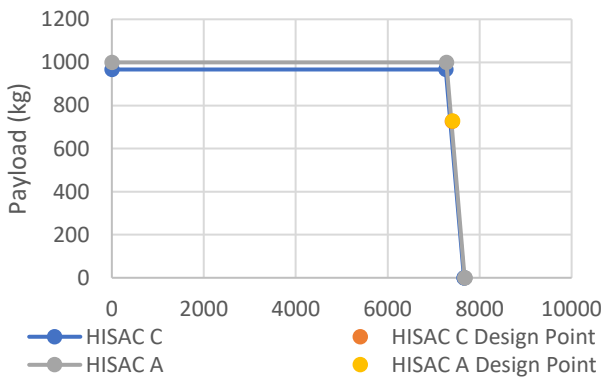


FIGURE 16: Payload-Range characteristics of HISAC A and HISAC C similar aircraft calculated by openAD

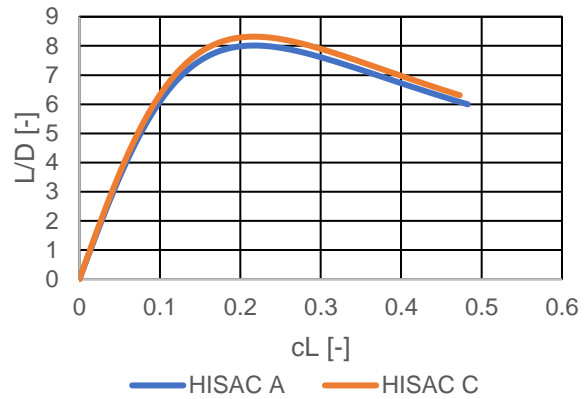


FIGURE 17: Aerodynamic polars of HISAC A and C similar aircraft calculated by openAD at mid cruise condition

As an experimental aircraft the X-59A represents a very different area of the design space with the aircraft characteristics displayed in TAB 3. It is chosen for reference purposes in the future. To the current state the number of published information is limited and older papers redesigning the X-59A do not display the current state. As shown in FIGURE 18 the configurations feature a three-surface aircraft with canards in front of the cockpit and a conventional VTP/HTP arrangement. The wing-fuselage connection is designed as a mid-wing with a noticeable inclination angle. The single engine is positioned in the back of the fuselage. Since no payload-range diagram or aerodynamic data are available a limited validation is performed via TAB 4.

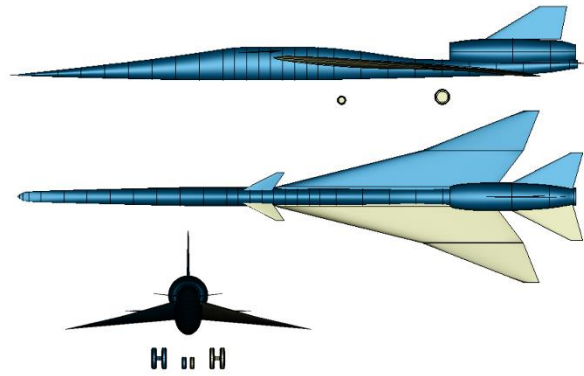


FIGURE 18: Three view X-59A similar aircraft

TAB 4: Verification of results using publicly available information

	Concorde		HISAC A		HISAC C		X-59A	
EM [kg]	74642	-1,00%	22537	-2,50%	25890	3,05%	6801	0,03%
OEM [kg]	76995	-0,96%	23465	-	26353	2,99%	7123	-
MTOM [kg]	180230	-2,68%	50376	0,00%	53429	0,24%	11341	0,02%
Fuel [kg]	93578	-2,25%	26463	-1,65%	26646	-2,45%	3946	0,00%
L/D [-]	7,3	2,74%	6,97	-0,43%	7,74	-1,84%	7,1	-

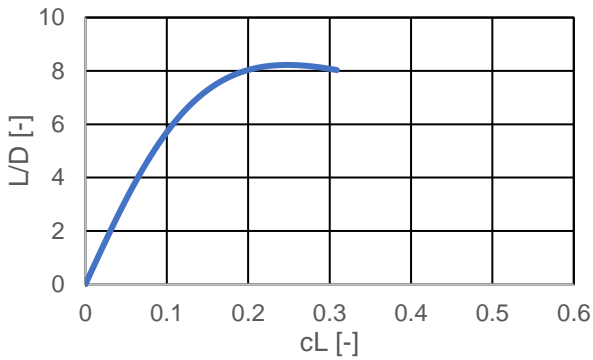


FIGURE 19: Aerodynamic polars of X-59A similar aircraft calculated by openAD at mid cruise condition

Across all design ranges, passenger capacities and Mach numbers of the design space the comparisons of the openAD results to the reference aircraft demonstrate a high level of accuracy. Besides the TLAR definition and configurational decisions, only little effort is needed to match the performance of the airliner, SSBJ and experimental aircraft. Adaptations and calibration of with, engine and aerodynamic performance methodologies are limited to a minimum set of parameters. The largest deviations are seen on the weights across all aircraft. This is mainly due to conditional architecture, which is unique to each design, naming the canard configuration of the HISAC A or the engine position of HISAC C, the single engine design of the X-59A or fuselage shapes in general. FIGURE 20 highlights the sensitivities of the Concorde similar aircraft based on the calculation methodologies implemented in openAD. The parameters specific fuel consumption (SFC), operating empty mass (OEM) and total drag (c_D) are varied by $\pm 5\%$. Within such a range, the influence is expected to be linear for smaller variations. The sensitivity study presented is independent from technology development and highlights the impact on aircraft level via block fuel changes. Generic factors are applied on aerodynamics, engine performance and weight parameters.

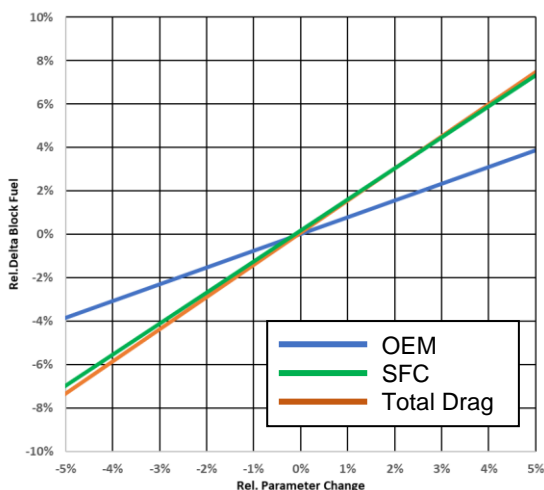


FIGURE 20: Impact of parameter variations of OEM, SFC and total drag (c_D) on block fuel for the Concorde similar aircraft calculated by openAD

For each parameter change, an entire sizing loop within

openAD is carried out, whereas all weight parameters, engine performance and aerodynamic behavior as well as the mission performance are recalculated. The sensitivity study identifies that the SFC variation results as the variation with the highest overall impact. By decreasing the SFC of the engine, the mission fuel requirement is reduced, and hence, due to the high fuel fraction reduces requirements on structure leading to less EM. Similar results are shown varying total drag. Thrust requirements are reduced and hence, a resized engine with less installed thrust is required. Significantly lower is the impact of mass. That lays within the general expectation for supersonic aircraft due to the high fuel fraction compared to subsonic aircraft.

5. CONCLUSION

OpenAD is mainly designed with the focus on modern standard airliner. That reflected in the selection of parameters and methodologies. OpenAD is designed for initiating consistent designs without being depended on disciplinary tools as well as supporting in a multifidelity and multidisciplinary design environment by activate and deactivate modules of the tool as well as provide the output in a CPACS compatible format. The object-oriented programming in python and the allocation of parameters to the main classes enable fast and flexible extensions to the knowledge base. It is developed with the use cases of today's common airliner in mind, with a range from 19 to 800 seats and a Mach numbers below Mach 1.0.

Extensive work is now invested into the development of the design capabilities in order to be able to create an overall supersonic aircraft design tool with a flexible and collaborative design approach in mind. It can not only be applied as a stand-alone tool for conceptual design studies but also in the DLR design environment to support more detailed design studies with higher-fidelity tools involved.

The work presented here highlights extension of openAD to supersonic aircraft design with a design space from 1 seater to 110-seater across a wide variety of use cases from airliner over business jets to experimental aircraft. The core principles of supersonic aircraft design are presented and the selected methodologies are presented. The verification of the tool via Concorde, HISAC A, HISAC C and X-59 shows consistent results and flexibility over a big range of use cases with varying mission profiles and cruise Mach numbers from Mach 1.2 to Mach 2.0.

This paper reflects the current state of supersonic conceptual aircraft design via openAD. Applied to ongoing and future projects, the tool is and will be under continuous development in order to widen and refine the design space.

6. ACKNOWLEDGMENT

The authors would like to thank Sebastian Wöhler and all colleagues involved in the development of supersonic capabilities for openAD.

7. REFERENCES

- [1] History.com Editors, "The Concorde makes its final flight," 2021 October 22. [Online]. Available: <https://www.history.com/this-day-in-history/the-concorde-makes-its-final-flight>. [Accessed 2022 January 27].
- [2] B. Liebhardt, K. Lütjens, A. Ueno and H. Ishikawa, "JAXA's S4 Supersonic Low-Boom Airliner – A Collaborative Study on Aircraft Design, Sonic Boom Simulation, and Market Prospects," in *AIAA AVIATION Forum*, Virtual Event, 2020.
- [3] F. Allroggen, "Market Potential for Commercial Supersonic Flight," in *AIAA SciTech*, 2022.
- [4] P. Krus and A. Abdallah, "Modelling of Transonic and Supersonic Aerodynamics for Conceptual Design and Flight Simulation," in *Aerospace Technology Congress*, Stockholm, Sweden, 2019.
- [5] Y.-L. Ding, Z.-H. Han, J.-L. Qiao, W.-P. Song and B.-F. Song, "Fast method and an integrated code for sonic boom prediction of supersonic commercial aircraft," in *ICAS Congress*, Shanghai, 2021.
- [6] K. F. Joiner, J. Zahra and O. Rehman, "Conceptual sizing of next supersonic passenger aircraft from regression of the limited existing designs," in *MATEC Web of Conferences*, 2018.
- [7] J. J. Berton, D. L. Huff, J. A. Seidel and K. A. Geiselhart, "Supersonic Technology Concept Aeroplanes for Environmental Studies," in *AIAA SciTech Forum and Exposition*, Orlando, Florida, 2020.
- [8] A. Abdalla, F. de Castro Baraky and M. Urzedo Quirino, "Conceptual design analysis of a variable swept half-span wing of a supersonic business jet," *CEAS Aeronautical Journal*, pp. 885-895, 01 December 2020.
- [9] Y. Sun and H. Smith, "Conceptual design of sonic boom stealth supersonic transports," *CEAS Aeronaut J* (2022). <https://doi.org/10.1007/s13272-021-00567-x>, 13 January 2022.
- [10] G. Carrier, J. Cadillon, P. Grenson, O. Atinault, M. Huet, F. Morel and S. Defoort, "Combined conceptual and preliminary aerodynamic design of a low-boom Supersonic Civil Transport aircraft for holistic evaluation of its environmental impact," in *AIAA AVIATION 2021 FORUM*, VIRTUAL EVENT, United States, 2021.
- [11] M. Nöding, M. Schuermann, L. Bertsch, M. Koch, M. Plohr, R. Jaron and J. Berton, "Simulation of Landing and Take-off Noise for Supersonic Transport Aircraft at a Conceptual Design Fidelity Level," *Aerospace*, pp. 1-23; 10.3390/aerospace9010009, January 2022.
- [12] J. P. Lawrence, R. J. Hutchinson and K. F. Joiner, "Conceptual aerodynamic design of an executive supersonic passenger aircraft – ESPA," *Proceedings of the Institution of Mechanical Engineers, Part G: Journal of Aerospace Engineering*, p. doi: 10.1177/09544100211025102., June 2021.
- [13] R. Seubert, "Validation of the Preliminary Aircraft Design and Optimization Program for Supersonic Commercial Transport Aircraft PrADO-Sup," in *DGLR-Fach-Symposium*, Berlin, 1998.
- [14] U. Hermann, "Multiple Discipline Optimization and Aerodynamic Off-Design Analysis of Supersonic Transport Aircraft," *Journal of Aircraft* 45(5), pp. 1474-1480, 2008.
- [15] B. Fröhler, D. Silberhorn, P. Balack, G. Atanasov, S. Wöhler, M. Iwanizki, J. Häßy, T. Zill and B. Nagel, "Advancement of the Conceptual Aircraft Design Tool openAD Applicable for Blended-Wing-Bodies within a Variable Fidelity MDAO Environment," in *ICAS Congress*, Stockholm, Sweden, 2022.
- [16] E. Torenbeek, *Synthesis of Subsonic*, Delft, Netherlands: Kluwer Academic Publishers, 1984.
- [17] J. Roskam, *Airplane Design, Part 1-7*, Lawrence, USA: Design, Analysis and Research, 1985.
- [18] "Luftfahrttechnisches Handbuch," 2018. [Online]. Available: <https://www.lth-online.de/>. [Accessed 2019].
- [19] D. P. Wells, B. L. Horvath and L. A. McCullers, "The Flight Optimization System - Weights Estimation Method," NASA Langley Research Center, Virginia, USA, 2017.
- [20] L. R. Jenkinson, P. Simpkin and D. Rhodes, *Civil Jet Aircraft Design*, United Kingdom: Butterworth Heinemann, 1999.
- [21] D. P. Raymer, *Aircraft Design: A Conceptual Approach*, Washington DC, USA: AIAA Education, 2012.
- [22] M. Alder, E. Moerland and J. Jepsen, "Recent advances in establishing a common language for aircraft design with CPACS," in *Aerospace Europe Conference*, Bordeaux, France, 2020.
- [23] S. Woehler, G. Atanasov, D. Silberhorn, B. Fröhler and T. Zill, *Preliminary Aircraft Design within a Multidisciplinary and Multifidelity Design Environment*, Bordeaux; France: Aerospace Europe Conference 2020, 2020.
- [24] Y. Sun and H. Smith, "Review and prospect of supersonic business jet design," *Progress in Aerospace Sciences - Volume 90*, pp. 12-38, April 2017.
- [25] O. Gonzalez-Gallego, R. E. Perez and P. W. Jansen, "Technical Viability and Operational Assessment of a Supersonic Business Jet," in *AIAA AVIATION Forum: Aviation Technology, Integration, and Operations Conference*, Atlanta, United States, 2018.

- [26] H. Jimenez and D. N. Mavis, "Conceptual Design of Current Technology and Advanced Concepts for an Efficient Multi-Mach Aircraft," *SAE Transactions*, no. 114, pp. 1343-1353, 2005.
- [27] "Civil Turbojet/Turbofan Specifications," [Online]. Available: <http://www.jet-engine.net/civtfspec.htm>. [Accessed 07 February 2022].
- [28] L. M. Nicolai and G. E. Carichner, *Fundamentals of Aircraft and Airship Design Volume I — Aircraft Design*, Reston, VA, United States: American Institute of Aeronautics and Astronautics, INC., 2010.
- [29] P. D.-I. R. Voit-Nitschmann, *Einführung in die Luftfahrttechnik*, Stuttgart, 2003.
- [30] S. Gudmundsson, *General Aviation Aircraft Design: Applied Methods and Procedures, Appendix C2: Design of Canard Aircraft*, Elsevier Inc., 2013.
- [31] S. Cacciola, C. E. D. Riboldi and M. Arnoldi, "Three-Surface Model with Redundant Longitudinal Control: Modeling, Trim Optimization and Control in a Preliminary Design Perspective," *Aerospace*, no. 8, p. 139, 021.
- [32] EASA, "Easy Access Rules for Large Aeroplanes (CS-25) (Amendment 26)," October 2021. [Online]. Available: <https://www.easa.europa.eu/downloads/129018/en>. [Accessed 09 February 2022].
- [33] D. Howe, *Aircraft Conceptual Design Synthesis*, London and Bury St Edmunds, UK: Professional Engineering Publishing Limited, 2000.
- [34] Premier Aviation (UK) Ltd, "AIRCRAFT CABIN COMPARISON CHART," [Online]. Available: <https://premieraviation.com/aircraft-cabin-comparison-chart/>. [Accessed 30 08 2022].
- [35] Heritage Concorde, "Concorde fuel system - General description," [Online]. Available: <https://www.heritageconcorde.com/fuelgeneral>. [Accessed 01 February 2022].
- [36] M. De Saint, "HISAC - T - 6 - 26 - 1," 2008.
- [37] Lockheed Martin-Skunk Works, "X-59 Quiet Supersonic Technology X-Plane," 2022. [Online]. Available: <https://www.lockheedmartin.com/content/dam/lockheed-martin/aero/documents/quietSuperSonic/P22-01661%20Product%20Card%20X-59.pdf>. [Accessed 22 09 2022].